



Original article

Novel antiviral benzofuran-transition metal complexes

Shadia A. Galal^{a,*}, Amira S. Abd El-All^a, Khaled H. Hegab^b, Asmaa A. Magd-El-Din^a, Nabil S. Youssef^b, Hoda I. El-Diwani^a^a Division of Pharmaceutical and Drug Industries, Department of Chemistry of Natural and Microbial Products, National Research Center, Dokki, Cairo 12622, Egypt^b Division of Inorganic Chemical Industries and Mineral Resources, Department of Inorganic Chemistry, National Research Center, Dokki, 12622, Cairo, Egypt

ARTICLE INFO

Article history:

Received 28 August 2009

Received in revised form

21 February 2010

Accepted 17 March 2010

Available online 27 March 2010

Keywords:

Benzofurans

Transition metal complexes

Antiviral activity

HIV and HIV-1 RT inhibitory activity

HCV NS3-4A protease inhibitor activity

ABSTRACT

(5-(1*H*-benzo[*d*]imidazol-2-yl)-1*H*-pyrrol-3-yl)(6-hydroxy-4,7-dimethoxybenzofuran-5-yl)methanone (**4**) and 3-(6-hydroxy-4,7-dimethoxybenzofuran-5-carbonyl)-6*H*-pyrimido[1,6-*a*]pyrimidine-6,8(7*H*)-dione (**5**) were synthesized by the reaction of 4,7-dimethoxy-5-oxo-5*H*-furo[3,2-*g*]chromene-6-carbaldehyde (**1**) with (1*H*-benzo[*d*]imidazol-2-yl)methanamine dihydrochloride and 4-amino-2,6-dihydropyrimidine, respectively, via ROR in the presence of alcoholic KOH. The metal complexes **6-9** of compound **4**; **H₂L¹** with (CuCl₂, FeCl₃, ZnCl₂, and LaCl₃) and the metal complexes **10-13** of compound **5**; **H₂L²** with (CuCl₂, FeCl₃, CoCl₂ and LaCl₃) were synthesized to form 1:1 or 1:2 (metal: ligand) complexes. The HIV inhibitory activity of all new compounds was tested. The EC₅₀ values showed that, all of tested compounds were more potent than **Ateviridine**. Moreover, the benzoimidazolopyrrole derivative **4** (EC₅₀ = 9 × 10⁻⁶ μM) had higher therapeutic index than the standard. The HIV-1 RT inhibitory activity showed that all of the tested compounds showed significant potency but none of them showed higher activity than **Ateviridine**. The HCV NS3-4A protease inhibitor activity of the tested compounds revealed that the complex formation had great positive effect on the bioactivity, where the Fe-complex **7** was the most potent compound with higher therapeutic index than **VX-950**, the standard. Also, the cytotoxicity of the synthesized compounds on hepatocyte cell line, showed that Cu-complex **10** was the most potent compound with potency nearly to that of the standard.

© 2010 Elsevier Masson SAS. All rights reserved.

1. Introduction

In a previous manuscript, a new class of highly potent antitumor and antiviral agents, having the benzofuran [1–7] skeleton related to heterocyclic moieties by a carbonyl group at the 5-position, was successfully discovered by Galal et al. [8]. This was quite evidence that hetero-moieties joined to the benzofuranlycarbonyl skeleton obtained via the ring opening reaction (ROR) of furochromones [9,10], mostly have positive effect on activity and selectivity. The HIV inhibitory activity of the previously synthesized compounds as **I–III** (c.f. Fig. 1), indicated that all the compounds were distinctly potent and the evaluation of hepatitis C virus (HCV) NS3-4A protease inhibitory activity showed that some of these compounds were significantly active.

The enzyme reverse transcriptase (RT) is used by retroviruses to transcribe their single-stranded RNA genome into single-stranded DNA and to subsequently construct a complementary strand of DNA, providing a DNA double helix capable of integration into

host cell chromosomes. Reverse transcriptase is multifunctional enzyme. This enzyme exhibits an RNA and DNA directed polymerase activity. In addition reverse transcriptase catalyzes the degradation of RNA in an RNA-DNA hybrid. Functional HIV1-RT is a heterodimer contains two domains, the N-terminal polymerase domain and the C-terminal RNase H domain [11]. Because of the importance of RT to HIV replication, inhibitors of this enzyme are potential therapeutic agents in the battle against HIV.

The NS3-4A serine protease of hepatitis C virus (HCV) is essential for viral replication and therefore has been one of the most attractive targets for developing specific antiviral agents against HCV. Functional HCV NS3-4A serine protease is a heterodimeric enzyme comprising the N-terminal domain of the NS3 protein as well as the NS4A protein. Fig. 2 shown the X-ray crystallographic structures of the HCV NS3-4A protease. Based on the enzyme features [12], there are three alternative strategies for developing inhibitors of the HCV serine protease were initially envisioned: tampering with the NS3/NS4A interaction, interfering with zinc binding and preventing substrate binding in the active site. However, the first two strategies are currently viewed as extremely difficult [13] and the development of active site inhibitors of the NS3-4A enzyme is considered the most promising approach.

* Corresponding author. Tel.: +20 233371718; fax: +20 233370931.

E-mail address: sh12galal@yahoo.com (S.A. Galal).

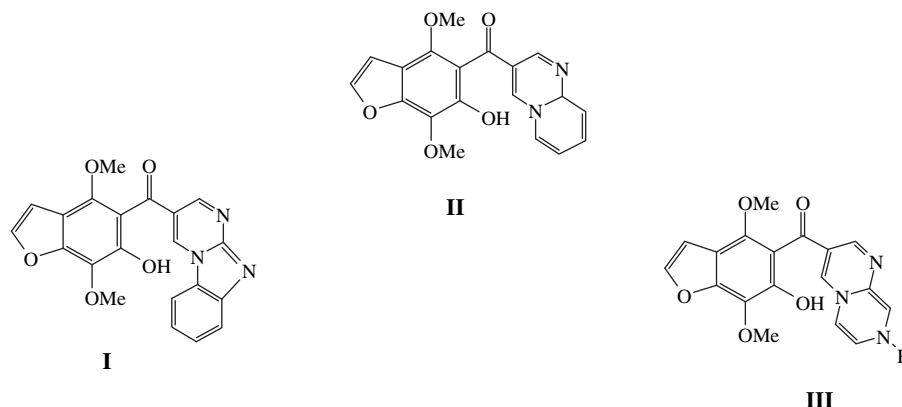


Fig. 1. Structural representations of potent antiviral benzofuran derivatives.

Our aim in this work was to design new ligands **4** and **5**, bearing good resemblance to the HIV reverse transcriptase inhibitor drug atevirdine and the protease inhibitor drug VX-950 (Fig. 3), and the formation of their transition metal complexes, aiming to study the HIV and HIV reverse transcriptase inhibitory activity besides the hepatitis C virus (HCV) NS3-4A protease inhibitory activity. Compounds **4** and **5** may serve as good ligands for transition metal ion due to the large conjugated pi-system, the azamethine nitrogen, the hydroxyl and the carbonyl groups which can positively affect the structures of the complexes. Where the unique redox and spectroscopic properties result in metal ions and their complexes

having potential medicinal applications that could be complementary to organic compounds [14].

2. Results and discussion

2.1. Chemistry

The reaction of 4,7-dimethoxy-5-oxo-5H-furo[3,2-g]chromene-6-carbaldehyde **1** [8,15,16] with (1H-benzimidazol-2-yl)methanamine dihydrochloride (**2**) [17] was previously studied by using a catalytic amount of triethyl amine or piperidine to give

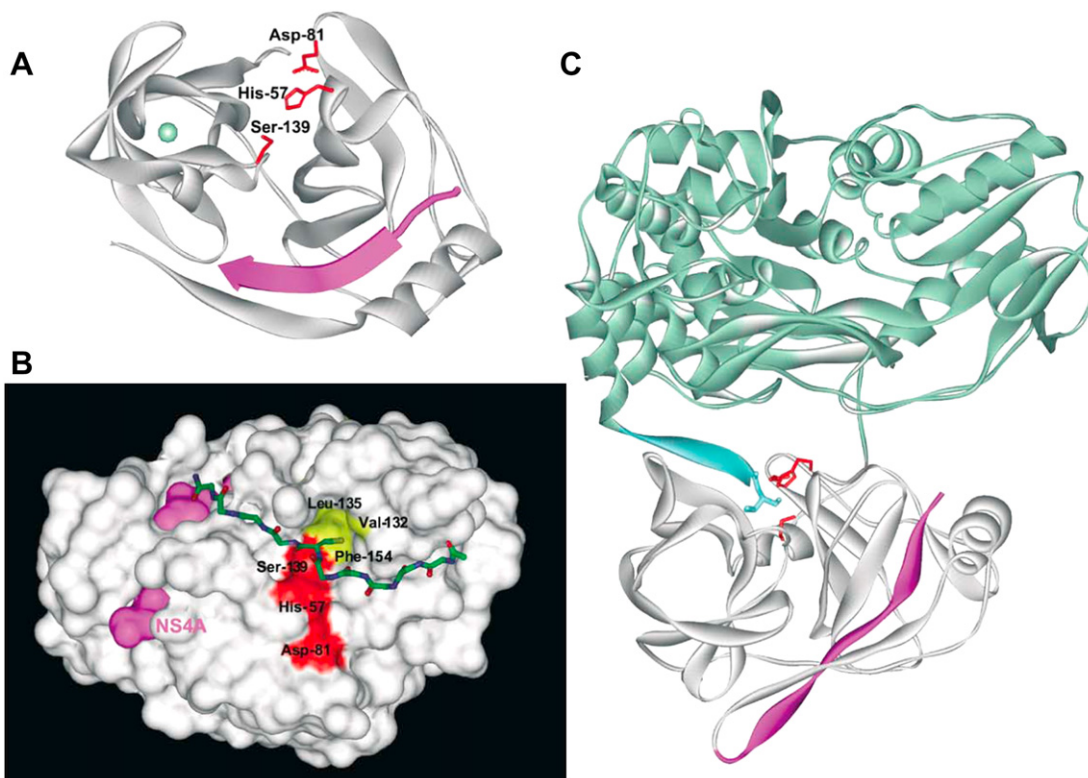


Fig. 2. X-ray crystallographic structures of the HCV NS3-4A protease. (A) NS3-4A protease domain. The side chains of the residues forming the catalytic triad (His-57, Asp-81, and Ser-139) are shown in red. The NS4A cofactor is shown in purple, the bound zinc ion is modeled in light green. (B) A decapeptide substrate (backbone only) is modeled in the NS3-4A protease active site. The NS4A cofactor is shown in purple. The side chains of the residues forming the catalytic triad are shown in red. The side chains of the residues forming the S1 specificity pocket of the enzyme (Val-132, Leu-135, and Phe-154) are shown in yellow. (C) Product inhibition in the NS3-4A complex. The NS4A peptide (red) has been artificially linked to the N-terminus of NS3 protease domain (gray) in the single-chain construct used for crystallization. The side chains of the residues forming the protease catalytic triad are shown in red. The helicase domain (top portion of the molecule) is depicted in light green. The C-terminus of NS3 generated as product of the NS3/NS4A cleavage reaction, forms a β -strand that occupies the proteinase active site (shown in light blue) (For interpretation of the references to color in this figure legend, the reader is referred to the web version of this article.).

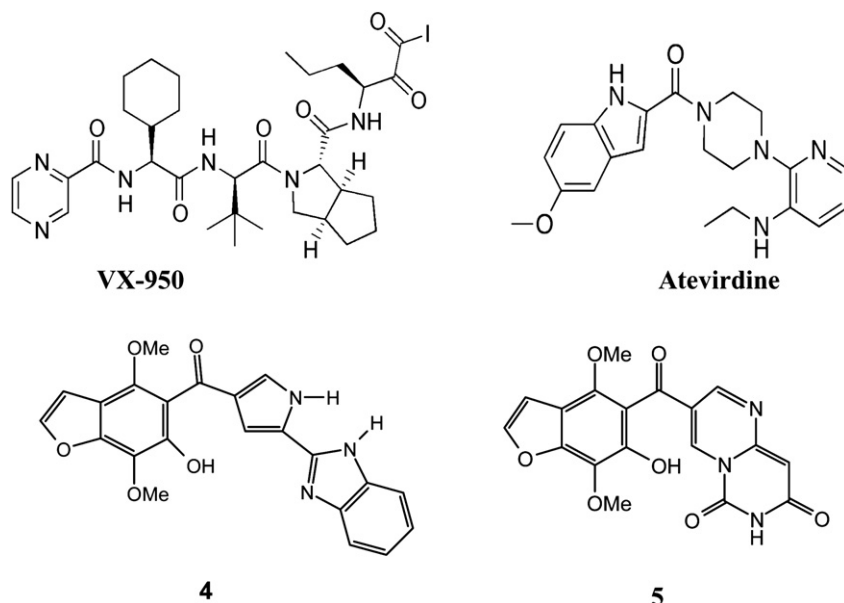


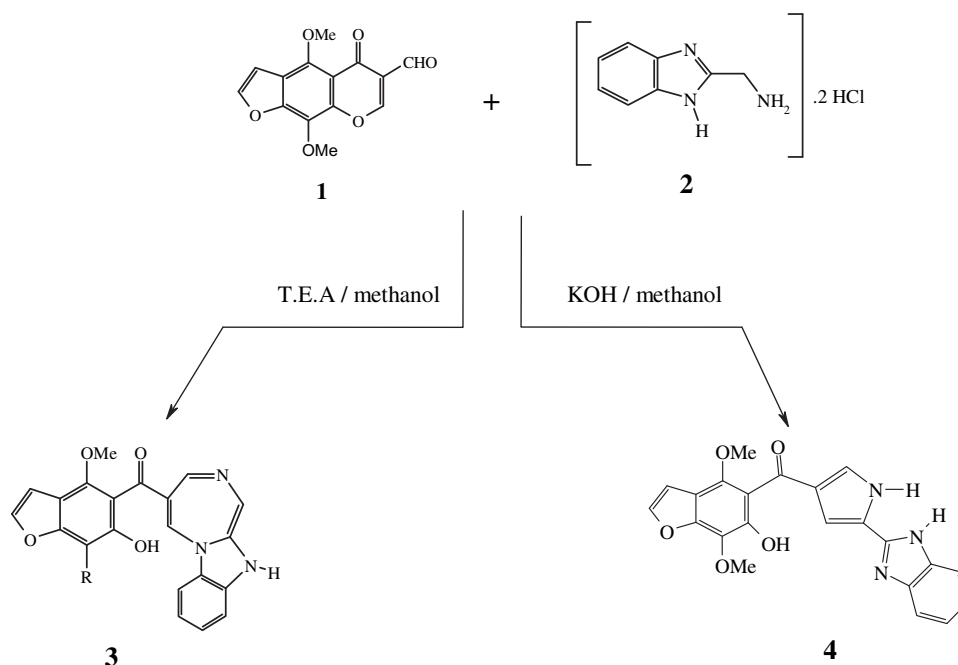
Fig. 3. The structure of Ateviridine, VX-950, compounds 4 and 5.

imidazodiazepine derivative **3** [8]. On the other hand, when potassium hydroxide is used as basic medium, benzimidazolylpyrrolyl derivative **4** was produced by the reaction of **1** and **2** (c.f. Scheme 1). The mass spectra and elemental analyses of both **3** and **4** showed that they have the same molecular weight but different melting points and R_f values. The $^1\text{H-NMR}$ spectrum of **4** showed the presence of some difference in the chemical shifts of both compounds as well as the presence of NH broad signal at δ 5.9 ppm exchangeable with D_2O . Besides, the IR spectrum of **4** revealed the NH band at 3230 cm^{-1} .

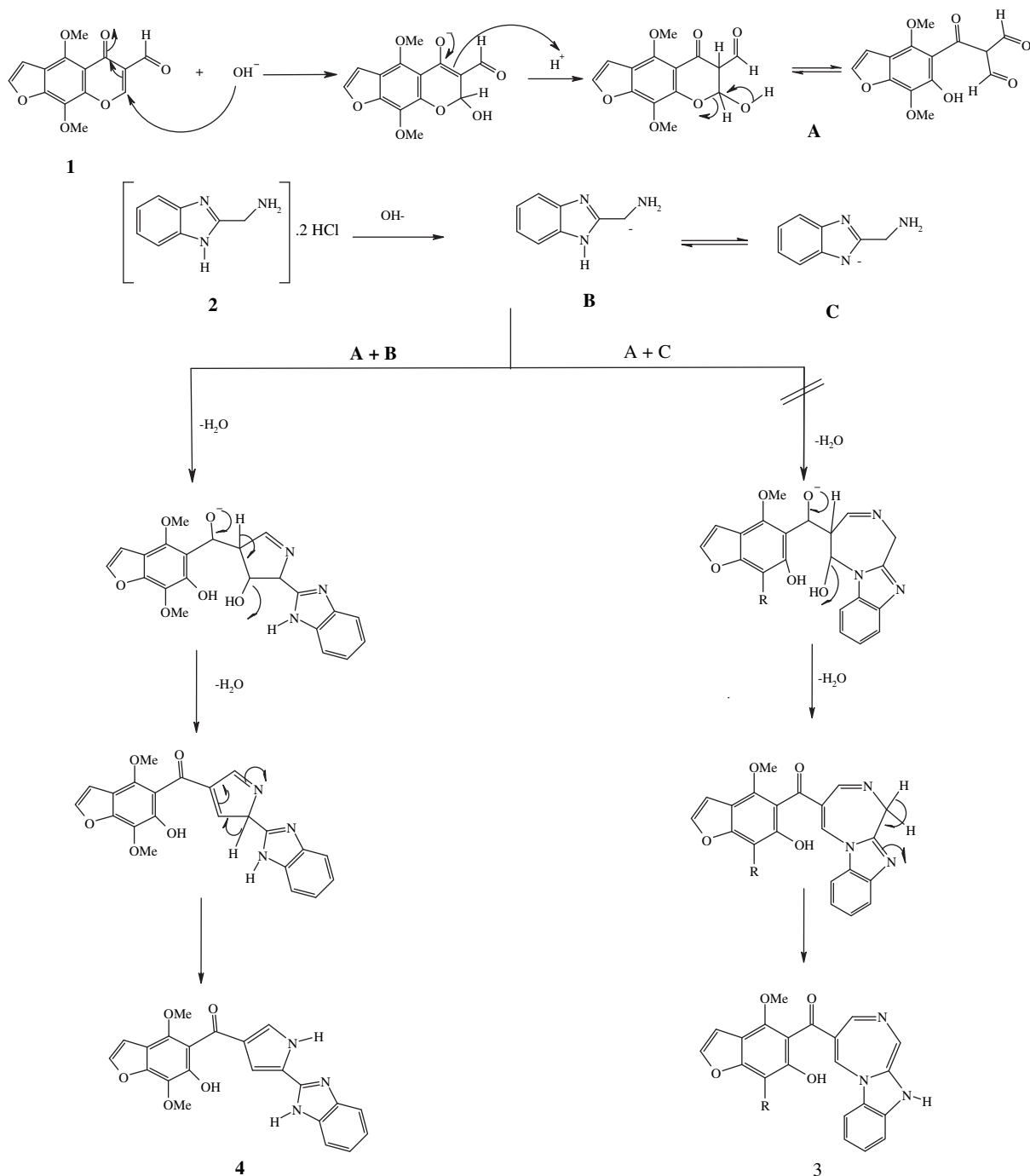
The suggested mechanism of the reaction of **1** and **2** in the presence of potassium hydroxide to afford **4** is explained in Scheme 2.

Reaction of 4-amino-2,6-dihydropyrimidine with compound **1** led to pyrimidopyrimidine derivative **5** (c.f. Scheme 3).

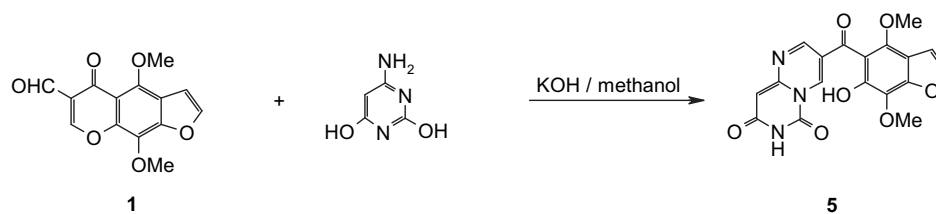
The metal complexes **6–9** of compound **4** with (CuCl_2 , FeCl_3 , ZnCl_2 , and LaCl_3) and the metal complexes **10–13** of compound **5** with (CuCl_2 , FeCl_3 , CoCl_2 and LaCl_3), respectively, were synthesized according to the reported methods by Merchán et al [18] to form 1:1 or 1:2 (metal: ligand) complexes. These complexes were characterized by elemental analyses, IR, $^1\text{H-NMR}$ and $^{13}\text{C-NMR}$ (for diamagnetic complexes), electronic and mass spectra, magnetic moments and conductance measurements as well as thermogravimetric analyses (TG). Based upon this characterization, the prepared complexes have the structural formulae: $[\text{Cu}(\text{HL}^1)(\text{H}_2\text{O})_4]\text{Cl}_2 \cdot 2\text{H}_2\text{O}$ (**6**), $[\text{Fe}(\text{HL}^1)\text{Cl}_2(\text{H}_2\text{O})_2] \cdot 2\text{H}_2\text{O}$ (**7**), $[\text{Zn}(\text{HL}^1)\text{Cl}(\text{H}_2\text{O})]$ (**8**), $[\text{La}$



Scheme 1. The reaction of 4,7-dimethoxy-5-oxo-5H-furo[3,2-g]chromene-6-carbaldehyde (**1**) and (1H-benzimidazol-2-yl)methanamine dihydrochloride (**2**) in basic medium.



Scheme 2. The suggested mechanism of the reaction of **1** and **2** in the presence of potassium hydroxide to afford **4**.

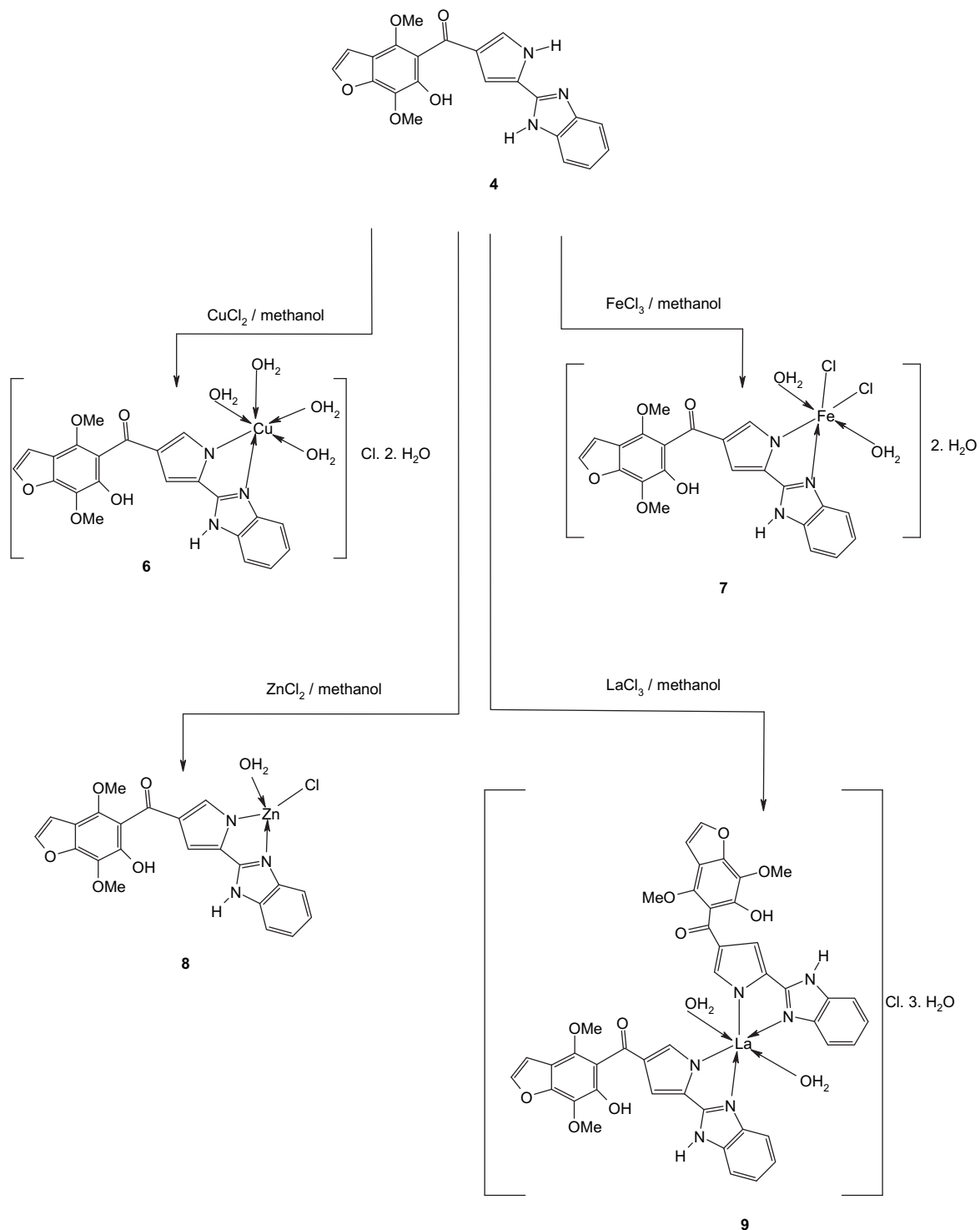


Scheme 3. The synthesis of pyrimidopyrimidine derivative **5**.

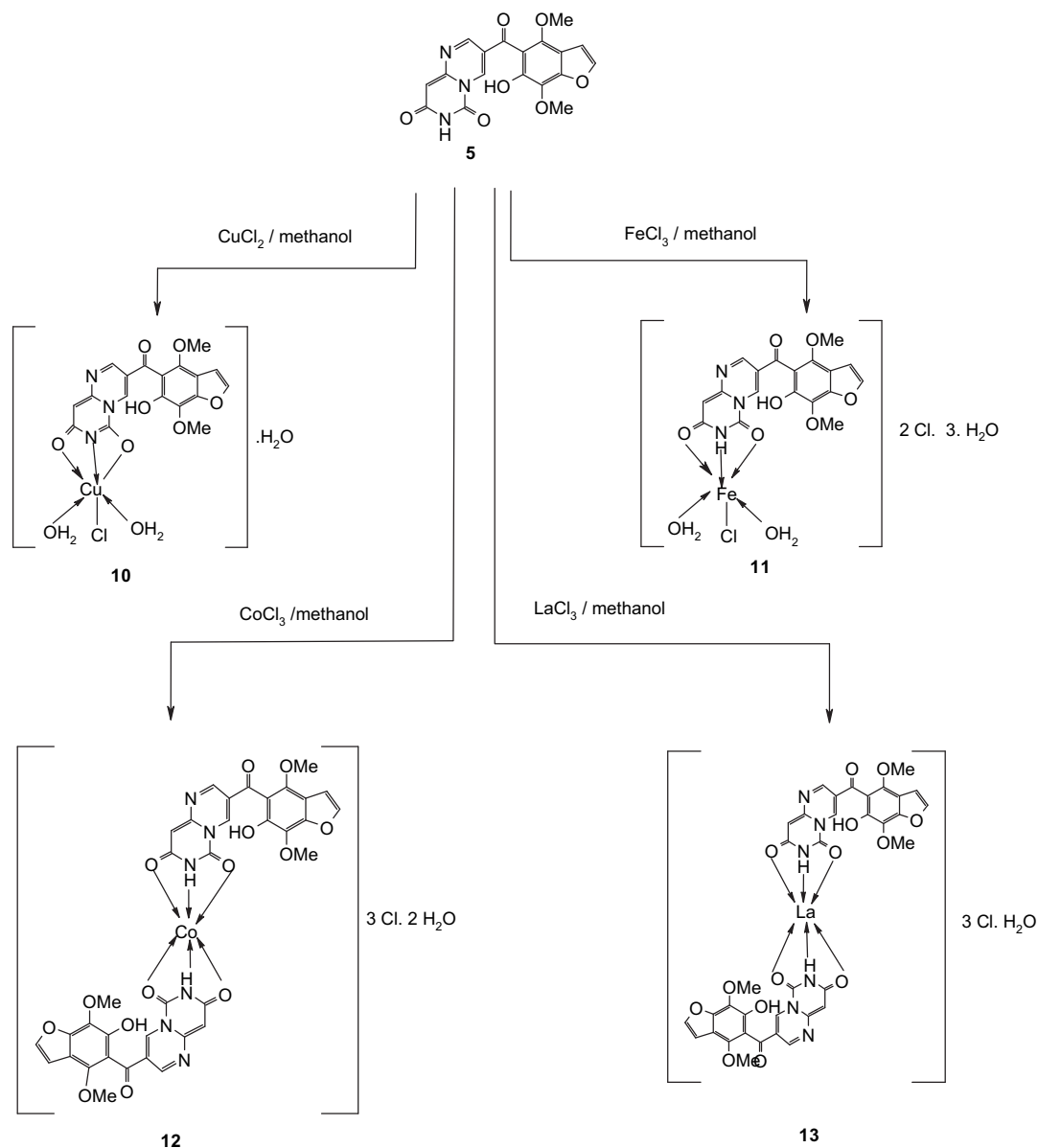
(HL¹)₂(H₂O)₂]Cl·3H₂O (**9**) for ligand **4**; H₂L¹ (c.f. Scheme 4). On the other hand, [Cu(HL²)Cl(H₂O)₂].H₂O (**10**), [Fe(H₂L²)Cl(H₂O)₂]·2Cl·3H₂O (**11**), [Co(H₂L²)₂]3Cl·2H₂O (**12**) and [La(H₂L²)₂].3Cl·H₂O (**13**) for ligand **5**; H₂L² (c.f. Scheme 5).

The IR broad bands in the range (3500–3200 cm⁻¹) indicated the presence of lattice water in the complexes **6–13** [19], which was further supported by the percents of weight loss observed from thermo-gravimetric analyses in the temperature range 25–204 °C

[20]. The bands due the stretching frequency of ν(C–O) and that of ν(C=O) groups were not greatly affected by complex formation in all complexes **6–13**, suggesting the non-bonding of these groups. For the complexes **6–9**, considerable frequency shifts of ν(C=N) in the wave numbers of the spectra of these complexes with respect to compound **4** were observed, which indicated the participation of azomethine nitrogen in the chelation of these complexes. The IR bands of complexes **11–13** showed that the two bands of the amide



Scheme 4. The synthesis of metal complexes **6–9** by coordination of compound **4** to CuCl₂, FeCl₃, ZnCl₂, and LaCl₃, respectively.



Scheme 5. The synthesis of metal complexes **10–13** by coordination of **5** to CuCl₂, FeCl₃, CoCl₂ and LaCl₃, respectively.

groups in the free ligand **5** at 1725 and 1662 cm⁻¹, were shifted to higher or lower wave numbers suggesting, the involvement of these groups in chelation. On the other hand, in the case of compound **10**, only one band appeared at 1696 cm⁻¹ due to amide group and a new band at 1274 cm⁻¹, due to ν(C–O), suggesting the chelation via carbonyl group and enolic (OH) groups of pyrimidine moiety. The FT-IR spectra of all chelates exhibited a band in the range of 590–670 cm⁻¹, assigned to ν(M–O). Also, new bands appeared at 485–491, 385–395 and 310–325 cm⁻¹ which may be due to ν(Cu–O), ν(Cu–N) and ν(Cu–Cl) for Cu–HL¹ and Cu–HL² complexes, respectively. In addition, two new bands displayed at 475 and 370 cm⁻¹ assignable for ν(Co–O) and ν(Co–N) in Co–H₂L² complex [21].

Upon coordination, the ¹H-NMR spectra of the complexes **8** and **9** with respect to the free ligand **4** showed that the exchangeable signal from NH of pyrrole moiety at 5.90 ppm, disappeared indicating the deprotonation of imino group due to Zn–N and La–N bond formation, respectively. Multiplets from H-5 and H-6 of benzimidazole and H-4 of pyrrole moieties in complexes **8** and **9**

were centered at 7.17 ppm. These signals were shifted towards lower frequencies, comparable to H-5 and H-6 at 7.50 ppm of benzimidazole moiety of compound **4**, giving coordination shifts Δ_{coord}: +0.33 ppm. Also, calculated coordination shifts Δ_{coord} of H-4 of pyrrole moiety: 7.63 ppm (for free ligand **4**) – 7.17 ppm (for complexes **8** and **9**) = +0.46. Furthermore, the multiplet at 7.75 ppm due to H-4 and H-7 in benzimidazole and H-2 in pyrrole moieties of compound **4** exhibited considerable chemical shifts upon coordination. H-4 in benzimidazole moiety shifted to 7.44 ppm in complex **8** and to 7.39 ppm in compound **9**, whereas H-7 in benzimidazole moiety showed lower field shift to 7.20 ppm in complex **8** and to 7.17 ppm in compound **9**. H-2 in pyrrole moiety of compound **4** signal shifted towards higher frequencies and appeared as singlet at 8.17 ppm for complex **8** and at 8.15 ppm for complex **9**, giving coordination shifts Δ_{coord}: –0.42 ppm and –0.40 ppm for compounds **8** and **9**, respectively. Moreover, exchangeable signal due to NH benzimidazole moiety in compound **4** appeared at 9.5 ppm was shifted to higher frequency, at 12.59 ppm and 11.90 ppm, respectively, due to coordination in both

Table 1The observed chemical shifts of some $^1\text{H-NMR}$ signals of free ligand **4** and its complexes **8** and **9**.

Compounds #	NH pyrrol	H5' and H6' Benzimi-dazole	H4'' pyrrol	H4 benzimi-dazole	H7 Benzimi-dazole	H2'' pyrrol,	NH benzimi-dazole
4	5.90	7.50	7.63	7.75	7.75	7.75	9.29
8	–	7.17	7.17	7.44	7.20	8.17	12.59
9	–	7.17	7.17	7.39	7.17	8.15	11.90

complexes **8** and **9**. The presence of the exchangeable protons (NH of benzimidazole and OH of hydroxy benzofuran) signals and the disappearance of (NH of pyrrole) signal was in agreement with the IR data of these complexes. Besides, the $^{13}\text{C-NMR}$ spectra of these complexes **8** and **9** showed strong chemical shifts of (C=N) signals upon coordination, from 148.76 ppm for the free ligand **4** to 155.76 ppm and 152.81 ppm for complexes **8** and **9**, respectively.

The $^1\text{H-NMR}$ spectra of the complexes **12** and **13** exhibited remarkable downfield shift of δ pyrimidopyrimidinone signals as well as high downfield shift of the exchangeable proton NH of pyrimidopyrimidinone at 11.67 ppm (for complex **12**) and 10.35 ppm (for complex **13**) compared to the free ligand **5** at 6.71 ppm. Also, the H-9' pyrimidopyrimidinone signal appeared at 8.23 ppm in free ligand **5** exhibited higher frequency shift at 8.93 ppm for complex **12** and lower frequency shift at 7.95 ppm for complex **13**. Furthermore, the H-2' pyrimidopyrimidinone signal appeared at 8.81 ppm in free ligand **5** exhibited higher frequency shift at 9.56 ppm for complex **12** and lower frequency shift at 8.42 ppm for complex **13**. On the other hand, the presence of the exchangeable proton (OH of hydroxy benzofuran) without notable shift with respect to compound **5** was in accordance with the IR data. Moreover, the $^{13}\text{C-NMR}$ of complexes **12** and **13** showed significant coordination shifts in C=O groups of pyrimidopyrimidinone. Calculated coordination shift Δ_{coord} of C=O: 148.86 ppm (for free ligand **5**) – 144.96 ppm (for complex **12**) = + 3.90 ppm, whereas the (C=O) signal appeared at 146.46 ppm for complex **9** upon coordination, with Δ_{coord} : +2.20 ppm. Tables 1 and 2 exhibited the remarkable chemical shifts of the $^1\text{H-NMR}$ signals of free ligands **4** and **5** and their diamagnetic complexes that affected by coordination.

The molar conductance of complexes **6**, **9** and **11–13** are around $67\text{--}85\ \Omega^{-1}\text{cm}^2\text{mol}^{-1}$, indicating the electrolytic nature of these complexes, whereas, **7**, **8** and **10** have molar conductance values of $16\text{--}28\ \Omega^{-1}\text{cm}^2\text{mol}^{-1}$, respectively, confirming their non-electrolytic nature [22].

The thermogravimetric data obtained were in a good agreement with the theoretical formulae as suggested from the elemental analyses.

The electronic transitions for **4** and **5** and their metal complexes, with their magnetic moments (B.M.) and the electronic of these complexes are studied (c.f. Table 3). The absorption spectra of the two ligands showed bands in the region 245–400 nm, which can be assigned to $\pi\text{--}\pi^*$ and $n\text{--}\pi^*$ transitions of the conjugated system. The spectra of compound **8** exhibited two bands at 293 and 350 nm which can be assigned to $\pi\text{--}\pi^*$ transition of the conjugated system and only one peak about 410 nm which can be attributed to MLCT ($d_M\text{--}\pi^*_L$), which confirming the tetrahedral structure of this complex. On the other hand, the Cu complexes **6** and **10** have magnetic moments 1.78–1.71 B.M., lying in the normal range

Table 2The observed chemical shifts of some $^1\text{H-NMR}$ signals of free ligand **5** and its complexes **12** and **13**.

Compounds #	NH	H9' pyrimido-pyrimidinone	H2' pyrimido-pyrimidinone
5	6.71	8.23	8.81
12	11.67	8.93	9.56
13	10.35	7.95	8.42

observed for octahedral Cu (II) complexes and corresponding to one unpaired electron, consequently confirming the monomeric nature of these complexes [23]. The observed magnetic moment of the complex **12** was 4.7 BM. The molar conductance of this complex in DMF is $79\ \Omega^{-1}\text{cm}^2\text{mol}^{-1}$, indicating the electrolytic nature of this complex. The electronic spectrum of this complex displayed two electronic spectral bands at 708 and 530 nm assignable to $^4\text{T}_{1g}(\text{F}) \rightarrow ^4\text{A}_{2g}(\text{F})$ and $^4\text{T}_{1g}(\text{F}) \rightarrow ^4\text{T}_{2g}(\text{P})$ transitions, respectively, characteristic of octahedral geometry [12]. In case of the Fe complexes **7** and **11**, the broad band's observed at 527–720 and 705–765, respectively, can be assigned to the $^6\text{A}_{1g} \rightarrow ^4\text{T}_{1g}(\text{G})$ and $^6\text{A}_{1g} \rightarrow ^4\text{T}_{2g}(\text{G})$ multiplicity forbidden transitions suggesting an octahedral field around iron (III) ion similar to other high spin d^5 -chelates [24]. The magnetic moment of this complex was 5.18 B.M.

2.2. Antiviral activity

2.2.1. HIV inhibitory activity and reverse transcriptase inhibition with therapeutic windows

Antiviral and toxicity data were reported as compound concentration required to inhibit the virus induced cell killing by 50%. (EC_{50}). The compounds **1**, **4–13** were tested for RT inhibitory activity against purified recombinant HIV-1 RT using the cell-free Quan-T-RT assay system (Amersham Corp., Arlington Heights, IL), which utilizes the scintillation proximity assay (SPA) principle [25,26]. $\text{IC}_{50[\text{RT}]}$ values (concentration at which the compound inhibits recombinant RT by 50%) were calculated by comparing the measurements to untreated sample [27]. Results of HIV and HIV-RT inhibitory activity of the tested compounds and Ateviridine, the standard drug used, were evaluated (c.f. Table 4).

The EC_{50} values listed in Table 4 showed that, the parent compound **1** ($\text{EC}_{50} = 2.0 \times 10^{-6}$), the free ligands **4** ($\text{EC}_{50} = 9 \times 10^{-6}\ \mu\text{M}$) and **5** ($\text{EC}_{50} = 10 \times 10^{-6}\ \mu\text{M}$) are more potent than Ateviridine ($\text{EC}_{50} = 10 \times 10^{-4}\ \mu\text{M}$). Moreover the benzimidazolylpyrrol derivative **4** has much better therapeutic index (TI = 110,000) than the standard drug (TI = 100,000). On the other hand, the complexes **6–13** and Ateviridine have comparable potency. Also, the complexes **6** (TI = 52, 665) and **13** (TI = 56, 234) presented relative interesting therapeutic index. Studying the bioactivity of new synthesized compounds indicated that the coordination of **4** and **5** to a transition metal ion to form the complexes **6–13** decrease the potency relatively.

Table 3Electronic Absorption Spectral Bands and Magnetic Moment of the Ligands **4** and **5** and their Complexes **6–13**.

Compounds #	Intraligand & Charge Transfer bands (nm)	d-d Bands (nm)	Magnetic Moment B.M.
4	295, 352, 360, 395	–	–
5	245, 260, 350, 400, 440	–	–
6	262, 289, 336, 363, 399, 443	530, 730	1.78
7	260, 277, 324, 398, 414	527, 720	1.68
8	293, 350, 400	–	Dia
9	290, 350, 400, 423	–	Dia
10	263, 291, 335, 354, 362, 385	530, 706, 735	1.71
11	260, 285, 330, 350, 362	705, 730, 765	1.70
12	263, 277, 289, 355, 364	530, 708, 735	4.7
13	268, 295, 350	500, 550	Dia

Table 4

The HIV inhibitory activity and HIV- reverse transcriptase inhibition with therapeutic windows of the tested compounds **1** and **4–13** and standard.

Compounds #	EC ₅₀ ^d /μM ^a	IC ₅₀ [RT]/μM ^b	Therapeutic index ^c
1	2.0 × 10 ⁻⁶	17.53	32 567
4	9 × 10 ⁻⁶	34.12	110 000
5	10 × 10 ⁻⁶	40.31	45 786
6	6.8 × 10 ⁻⁴	87.98	52 665
7	7.1 × 10 ⁻⁴	90.17	12 768
8	8.5 × 10 ⁻⁴	92.27	23 498
9	5.5 × 10 ⁻⁴	82.27	43 498
10	3.1 × 10 ⁻⁴	80.16	22 567
11	5.4 × 10 ⁻⁴	90.31	44 324
12	6.5 × 10 ⁻⁴	96.18	23 458
13	2.1 × 10 ⁻⁴	78.67	56 234
Ateviridine	10 × 10 ⁻⁴	10	100 000

^a Compound concentration required to inhibit the virus induced cell killing by 50%.

^b Compound concentration required to achieve 50% inhibition of recombinant HIV-RT activity.

^c A therapeutic index is the lethal dose of a drug for 50% of the population (LD₅₀) divided by the minimum effective dose for 50% of the population (ED₅₀). (LD₅₀) is the dose required to kill half the members of the tested population. (ED₅₀) is the dosage that produces a desired effect in half the test.

^d EC₅₀ & IC₅₀ values were estimated by logistic regression analysis. One way ANOVA (P < 0.01) was used to test treatment difference in EC₅₀ & IC₅₀. After significant factor by ANOVA, individual group differences were analyzed using Holm-Sidak's procedure for multiple comparisons versus control.

Screening of HIV-1 reverse transcriptase inhibition of the synthesized compounds showed that the starting material, furochromone derivative **1**, was the most potent compound with lowest IC₅₀ (17 μM). This potency was correlated by high HIV activity. Also compound **4** showed high potency against HIV-1 reverse transcriptase inhibition activity with IC₅₀ = 34.12 μM, that was paralleled by its potent HIV activity, as the therapeutic index. This feature made compound **4** very interesting candidate for *in vivo* study. Furthermore, compound **5** showed high activity toward HIV-1 reverse transcriptase inhibition with IC₅₀ = 40.31 μM. Upon coordination of compound **4** and **5** to transition metal ions as Cu(II), Fe(III), Zn(II), Co (II) or La(II) to form the complexes **6–13**, The HIV-1 reverse transcriptase inhibition activity decreased which was also paralleled by HIV inhibitory activity reduction.

From the above screening of HIV-1 reverse transcriptase inhibitory activity with the HIV activity, the synthesized compounds showed high efficacy in inhibition of HIV reverse transcriptase enzyme which is the enzyme responsible about for viral replication.

The activity of the potent complexes may be due to intercalation of the metals with the DNA of the virus and hence inhibit its replication. Also, the activity indicates that the complexes have a suitable molecular size and stereochemistry so that metal ions can bind to the enzyme at its active site.

2.2.2. Hepatitis C virus (HCV) NS3-4A protease inhibitor activity

The development of potent competitive inhibitors of the HCV serine protease and identification of non-peptidic small molecule inhibitors of NS3-4A enzyme is significantly important. Studying of the hepatitis C virus (HCV) NS3-4A protease inhibitor activity of the compounds **1**, **4–13** was performed. For comparison, the non-covalent peptidomimetic NS3-4A protease inhibitor, **VX-950** was used as standard drug. The cytotoxicity of the tested compounds was measured under the same experimental settings using a tetrazolium (MTS)-based cell viability assay (Promega, Madison, WI). Cells were identical in sequence as described by Lohmann et al. [28]. Determination of 50% inhibitory concentration (IC₅₀), 90% inhibitory concentration (IC₉₀), and 50% cytotoxic concentration (CC₅₀) of all the tested compounds in HCV replicon cells was performed using a quantitative RT-PCR (QRT-PCR) assay [29,30]. The results of HCV NS3-4A protease inhibitor activity and the cytotoxic activity of the tested compounds and standard were listed (c.f. Table 5)

Screening of the 90% inhibitory concentration (IC₉₀) values revealed that all of the synthesized compounds have potent activity. The Fe-complex **7** (IC₉₀ = 0.345 ± 0.01 μM) was more potent than the standard drug, **VX-95**, (IC₉₀ = 0.45 ± 0.0003 μM) and its free ligand **4** (IC₉₀ = 1.654 ± 0.14 μM) besides the parent compound **1** (IC₉₀ = 0.796 ± 0.08 μM). Interestingly, compound **7** exhibited also wider therapeutic index than **VX-950** (TI = 1200) and compound **4** (TI = 462.52) besides compound **1** (TI = 555.82). Also, the Zn complex **8** (IC₉₀ = 1.23 ± 0.12 μM) and La complex **9** (IC₉₀ = 1.32 ± 0.13 μM) have higher potency than the ligand **4**. Whereas, the Cu complex **6** (IC₉₀ = 1.8 ± 0.09 μM) has less potency than **4**. By comparing the efficacy of complex formation **6–9** in the inhibition of hepatitis C virus (HCV) NS3-4A protease with respect to their free ligand **4**. The octahedral geometrical structure with of Fe-complex **7** is the most potent one, followed by the square planar Zn complex **8** then octahedral La complex **9** and finely the octahedral Cu complex **6**.

Furthermore, the pyrimidopyrimidine derivative **5** (IC₉₀ = 0.844 ± 0.07 μM) and the Cu complex **10** (IC₉₀ = 0.876 ± 0.09 μM) have convergent potent activity, but the Co complex **12**

Table 5

HCV NS3-4A protease inhibitory activity and the cytotoxic activity of the tested compounds (**1** and **4–13**) and standard.

Compounds #	IC ₅₀ ^a (±SD) ^f μM After 48 Hours	IC ₉₀ ^b (±SD) ^f μM After 48 Hours	CC ₅₀ ^c (±SD) ^f μM	Therapeutic index ^d
1	0.421 ± 0.03	0.796 ± 0.08	234 ± 5	555.82
4	0.657 ± 0.05	1.654 ± 0.14	765 ± 22	462.52
5	0.388 ± 0.04	0.844 ± 0.07	341 ± 8	878.87
6	0.432 ± 0.04	1.8 ± 0.09	256 ± 10	592.59
7	0.112 ± 0.01	0.345 ± 0.01	345 ± 17	3080.36
8	0.643 ± 0.04	1.23 ± 0.12	223 ± 11	346.81
9	0.564 ± 0.04	1.32 ± 0.13	234 ± 6	414.89
10	0.445 ± 0.034	0.876 ± 0.09	93 ± 10	208.99
11	0.987 ± 0.09	1.98 ± 0.09	330 ± 13	348.53
12	0.456 ± 0.05	0.987 ± 0.08	154 ± 12	337.72
13	0.765 ± 0.07	1.78 ± 0.09	213 ± 12	278.43
VX-950^e	0.20 ± 0.0001	0.45 ± 0.0003	90 ± 1.20	1200

^a Compound concentration required to achieve 50% inhibition of HCV NS3-4A protease activity.

^b Compound concentration required to achieve 90% inhibition of HCV NS3-4A protease activity.

^c Compound concentration required to reduce the cell viability by 50% as determined by MTT method.

^d A therapeutic index is the lethal dose of a drug for 50% of the population (LD₅₀) divided by the minimum effective dose for 50% of the population (ED₅₀). (LD₅₀) is the dose required to kill half the members of the tested population. (ED₅₀) is the dosage that produces a desired effect in half the test.

^e The standard used in comparison.

^f Data expressed as means ± SD for three independent experiments.

Table 6
The median lethal dose of the tested compounds (**1** and **4–13**).

Compound no.	(LD ₅₀ ^a ± SD ^b) ^c mg/kg
1	113.29 ± 1
4	166.15 ± 1
5	152.23 ± 1
6	169.4 ± 2
7	256 ± 2
8	263 ± 2
9	225.98 ± 1
10	416.18 ± 8
11	248 ± 2
12	243 ± 2
13	516 ± 5

^a Dose required to kill half the members of the tested population.

^b Data expressed as means ± SD for three independent experiments.

^c The median lethal dose of the tested compounds was determined according to the procedure described by Lorke.

(IC₉₀ = 0.987 ± 0.08 μM), La complex **13** (IC₉₀ = 1.23 ± 0.12 μM) and Fe-complex **11** (IC₉₀ = 1.98 ± 0.09 μM) exhibited lower potency than **5**. Regarding to the cytotoxicity of the synthesized compounds on hepatocyte cell lines, the Cu complex **10** (CC₅₀ = 93 ± 10 μM) is the most potent compound. The Co complex **12** (CC₅₀ = 154 ± 12 μM), La complex **13** (CC₅₀ = 213 ± 12 μM) and Fe-complex **11** (CC₅₀ = 330 ± 13 μM) have higher potency than their corresponding ligand **5**. This increased potency was not paralleled by higher inhibitory concentration (IC₅₀), as the therapeutic index. On the other hand, the complexes **6–9** have higher bioactivity than the ligand **4**. This increased potency was paralleled by higher inhibitory concentration (IC₅₀) (c.f. Table 5). The activity of the prepared complexes may be attributed to the binding of the metal ion with the active site of the NS3-4A enzyme.

2.3. The median lethal dose (LD₅₀)

The median lethal dose (LD₅₀) which is the dose of the tested compounds required to kill half the members of the tested population was determined according to the procedure described by Lorke [31–33]. The results of the LD₅₀ in mg/kg of the synthesized compounds were listed (c.f. Table 6). Screening the median lethal dose (LD₅₀) of the tested compounds **1**, **4–13** showed that, all the compounds were found to have higher LD₅₀ than compound **1**. These results indicated that the heteromoieties included into benzofuran skeleton decreased the toxicity of starting material **1** (LD₅₀ = 113.29 ± 1 mg/kg). Screening of LD₅₀ of the synthesized complexes with respect to their free ligand indicated that, complexes **8** (LD₅₀ = 263 ± 2 mg/kg), **7** (LD₅₀ = 256 ± 2 mg/kg) **9** (LD₅₀ = 225.98 ± 1 mg/kg), and **6** (LD₅₀ = 166.15 ± 1 mg/kg), respectively, have higher LD₅₀ than compound **4** (LD₅₀ = 166.15 ± 1 mg/kg). Moreover, complex **13** showed highest median lethal dose (LD₅₀ = 516 ± 5 mg/kg), followed by **10** (LD₅₀ = 416.18 ± 8 mg/kg), **11** (LD₅₀ = 248 ± 2 mg/kg), and **12** (LD₅₀ = 243 ± 2 mg/kg) and compound **5** (LD₅₀ = 152.23 ± 1 mg/kg). So the coordination of compound **4** and **5** to transition metal ion to form the complexes **6–13** have positive effect on the reduction of toxicity with respect to the free ligands **4** and **5**.

3. Conclusion

The reaction of 5-oxo-5H-furo[3,2-g]chromene-6-carbaldehydes **1** with (1H-benzimidazol-2-yl)methanamine dihydrochloride (**2**) was reliant on the reaction conditions and the mechanism of reaction had been suggested.

New potent antiviral benzofuran derivatives **4** and **5** besides, new potent complexes formed by the coordination of **4** and **5** to

a transition metal ion as Cu(II), Fe(III), Zn(II), Co (II) or La(II). The HIV inhibitory activity of the tested compounds were more potent than Ateviridine. Moreover, compound **4** had much better therapeutic index than the standard and its derived complexes **6–9**. On the other hand, the HIV-1 reverse transcriptase inhibition of the synthesized compounds showed significant potency but none of them showed higher activity than the standard. The HCV-NS3-4A protease inhibitor activity of the tested compounds showed high potency. The complex formation positively affected the bioactivity; furthermore, the Fe-complex **7** was the most potent compound with higher therapeutic index than the standard drug. Also, the cytotoxicity of the synthesized compounds on hepatocyte cell line, showed that Cu complex **10** was the most potent compound having almost the same potency as **VX-950**. Studying the median lethal dose LD₅₀ showed that the complex formation have positive effect on the reduction of toxicity of free ligands **4** and **5**. These features transform them in interesting candidate to further *in vivo* testing.

4. Experimental

4.1. Physical measurements

Microanalyses of the ligands and complexes were performed in the Microanalytical Laboratory Center, Faculty of Science, Cairo University, Egypt. Molar conductance was measured at room temperature on electronic conductivity model 19000-05 (USA). The IR spectra (4000–400 cm⁻¹) were recorded using KBr pellets in a Jasco FT/IR 300E Fourier transform infrared spectrophotometer and in the 500–100 cm⁻¹ region using Polyethylene-Sandwiched Nujol mulls on a Perkin Elmer FT-IR 1650 (spectrophotometer). The ¹H and ¹³C NMR spectra were recorded using Joel EX-270 MHz and 500 MHz NMR spectrophotometers. The electronic absorption spectra were recorded using a Shimadzu UV-240 UV-Visible recording spectrometer. The mass spectra were carried out using Finnigan mat SSQ 7000 (Thermo. Inst. Sys. Inc., USA) spectroscopy at 70 eV. Thermo-gravimetric analyses were carried out using a DTA-7 and TGA-7 perkin Elmer 7 series thermal analyses system. The magnetic moments were measured using Gouy method with Hg[Co(SCN)₄] as calibrant.

4.1.1. Preparation of ((1H-benzo[d]imidazol-2-yl)methanamine) dihydrochloride (**2**) [17]

A solution of glycine (150 mmol) and *o*-phenylenediamine (100 mmol) were refluxed in 5.5 N hydrochloric acid (100 mL) for 30 h. After the reaction mixture was left overnight, the hydrochloride salt was removed as white crystals which recrystallized from ethanol. Yield 89%, m.p. 263–265 °C (dec.) (lit. m.p. 263–265 °C dec.). ¹H-NMR (270 MHz, DMSO-*d*₆): 4.55 (s, 2H, CH₂), 4.96 (br., NH₂, D₂O exchangeable), 7.49(m, 2H, H4 and H7 benzimidazole), 7.79(m, 2H, H5 and H6 benzimidazole), 9.11(br., NH, D₂O exchangeable). ¹³C-NMR (270 MHz, DMSO-*d*₆): 34.54, 114.47, 126.11, 131.34, 146.90. IR (cm⁻¹): 3492.45(NH benzimidazole), 3288, 3208, 3157 (NH₂), 3052-2596 (br., CH (aromatic, aliphatic) and intermolecular H bonded NH), 1624.73(C=N), 1588, 1573 (C=C). MS: m/z 220 (M⁺, 0.3%), 147 (M⁺ - 2HCl, 100%).

4.1.2. Preparation of (11H-benzo[4,5]imidazo[1,2-a][1,4]diazepin-4-yl)(6-hydroxy-4,7-dimethoxy-benzofuran-5-yl)methanone (**3**) [8]

A mixture of 4,7-dimethoxy-5-oxo-5H-furo[3,2-g]chromene-6-carbaldehyde (**1**)^{13,14} (100 mmole), compound **2** (100 mmole) and triethylamine or piperidine (few drops) in methanol (60 mL) was refluxed for 7 h. The reaction mixture was filtered off and crystallized from DMF/methanol to give **3**. Yield: 83%, m.p. 315–317 °C. ¹H-NMR (500 MHz, DMSO-*d*₆): 3.94(s, 3H, CH₃), 4.0

(s, 3H, CH₃), 7.14(d, 1H, *J* = 1.5 Hz, H3 benzofuran), 7.47 (m, 2H, H9' and H10' benzimidazodiazepine), 7.56(d, 1H, *J* = 1.5 Hz, H2 benzofuran), 7.72(m, 4H, H2', H6', H8' and H11' benzimidazodiazepine), 7.91 (s, 1H, H4' benzimidazodiazepine), 9.23(br., NH, D₂O exchangeable), 12.75(s, 1H, OH, D₂O exchangeable), IR (KBr, ν/cm^{-1}): $\nu(\text{OH})$ 3503, $\nu(\text{NH})$ 3415, $\nu(\text{CH, aromatic})$ 3064, $\nu(\text{CH, aliphatic})$ 2970, $\nu(\text{intermolecular H bonded OH and NH})$ 3164–2655s, $\nu(\text{C=O})$ 1641s, $\nu(\text{C=N})$ 1608 m, $\nu(\text{C=C})$ 1540 m. MS: *m/z* 403 (M⁺, 45%), 220 (m₁, 100%), 183 (m₂, 93%), Anal. Calcd for C₂₂H₁₇N₃O₅: C, 65.50; H, 4.25; N, 10.42; Found: C, 65.40; H, 4.19; N, 10.30.

4.1.3. Preparation of compounds **4** and **5**

General Procedure: A mixture of 4,7-dimethoxy-5-oxo-5H-furo[3,2-g]chromene-6-carbaldehyde (**1**) (100 mmole), potassium hydroxide (100 mmole) in methanol (80 mL) and compound **2** or 4-amino-2,6-dihydropyrimidine (100 mmole) was refluxed. After the reaction completion, the reaction mixture was filtered off and crystallized from DMF/methanol to give **4** and **5**, respectively.

4.1.4. (5-(1H-benzofurimidazol-2-yl)-1H-pyrrol-3-yl)(6-hydroxy-4,7-dimethoxybenzofuran-5-yl)methanone (**4**)

Yield: 73%, m.p. 285–287 °C. ¹H-NMR (500 MHz, DMSO- *d*₆): 3.91(s, 3H, CH₃), 3.97(s, 3H, CH₃), 5.90(br, NH pyrrol, D₂O exchangeable), 7.17(d, 1H, *J* = 1.5 Hz, H3 benzofuran), 7.50(m, 2H, H5' and H6' benzimidazole), 7.63(s, 1H, H4'' pyrrol), 7.75(m, 3H, H2'' pyrrol, H4 and H7 benzimidazole), 7.94 (d, 1H, *J* = 1.5 Hz, H2 benzofuran), 9.29(br, NH benzimidazole D₂O exchangeable), 13.02 (s, 1H, OH, D₂O exchangeable). ¹³C-NMR(500 MHz, DMSO- *d*₆): 61.03 (OCH₃), 61.47 (OCH₃), 106.04, 112.18, 114.08, 115.91, 118.03, 118.24, 125.91, 129.142, 129.20, 131.28, 132.17, 142.99, 144.36, 144.81, 145.36, 148.76(C=N), 188.37(C=O). IR (ν/cm^{-1}): $\nu(\text{OH})$ 3520br., $\nu(\text{NH})$ 3415br., $\nu(\text{NH})$ 3230, $\nu(\text{CH, aromatic})$ 3064 m, $\nu(\text{CH, aliphatic})$ 2970, $\nu(\text{intermolecular H-bonded OH and NH})$ 3200–2655, $\nu(\text{C=O})$ 1641s, $\nu(\text{C=N})$ 1628 m, $\nu(\text{C=C})$ 1539 m, $\nu(\text{C-O})$ 1263s. MS: *m/z* 403(M⁺, 6.5%), 372(m₁, 5.64%), 220(m₂, 100%), 183 (m₃, 98%), Anal. Calcd for C₂₂H₁₇N₃O₅: C, 65.50; H, 4.25; N, 10.42; Found: C, 65.37 H, 4.17; N, 10.48.

4.1.5. 3-(6-hydroxy-4,7-dimethoxybenzofuran-5-carbonyl)-6H-pyrimido[1,6-a]pyrimidine-6,8(7H)-dione (**5**)

Yield: 88%. 290–292 °C. ¹H-NMR (270 MHz, DMSO- *d*₆): 3.85 (s, 3H, OCH₃), 3.93(s, 3H, OCH₃), 6.71(s, 1H, NH, D₂O exchangeable), 7.13(d, 1H, *J* = 2 Hz, H3 benzofuran), 7.96(d, 1H, *J* = 2 Hz, H2 benzofuran), 8.15(s, 1H, H4' pyrimidopyrimidinone), 8.23(s, 1H, H9' pyrimidopyrimidinone), 8.81(s, 1H, H2' pyrimidopyrimidinone), 9.89 (s, 1H, OH, D₂O exchangeable), 12.16(s, 1H, OH, D₂O exchangeable). ¹³C-NMR(270 MHz, DMSO- *d*₆): 61.31, 60.83, 105.56, 108.20, 109.69, 110.87, 111.45, 112.12, 114.47, 127.12, 128.39, 136.50, 137.76, 143.23, 144.01, 144.63, 144.92, 145.68, 148.86(C=O), 153.56, 157.15, 158.23(C=N), 165.44 (C=O), 191.23 (C=O, ketone). (KBr, ν/cm^{-1}): $\nu(\text{OH})$ 3577, $\nu(\text{NH})$ 3414br., $\nu(\text{CH, aromatic})$ 3164 m, $\nu(\text{CH aliphatic})$ 2992 m, $\nu(\text{C=O})$ 1725s, $\nu(\text{C=O})$ 1662s, $\nu(\text{C=O})$ 1640s, $\nu(\text{C=N})$ 1605s, $\nu(\text{C=C})$ 1542 m, $\nu(\text{C-O})$ 1213s. MS: *m/z* 383 (M⁺, 100%). Anal. Calcd for C₁₈H₁₃N₃O₇: C, 56.40; H, 3.42; N, 10.96. Found: C, 56.21; H, 3.88; N, 10.89.

4.1.6. Preparation of the metal complexes (**6**–**13**)

General procedure: A solution of the metal ion in ethanol was added to a solution of the corresponding ligand in ethanol to form 1:1 or 1:2 M: L complexes. The reaction mixture was heated under reflux temperature, after reaction completion. The resulting precipitates were filtered off, washed with diethyl ether followed by hot ethanol. Then, recrystallized from methanol/DMF. All of the complexes decomposed without melting with m.p. >300 °C.

4.1.7. (2-(1H-benzofurimidazol-2-yl)-4-(6-hydroxy-4,7-dimethoxybenzofuran-5-carbonyl)-1H-pyrrol-1-yl)copper(II) chloride hexahydrate; [Cu(HL¹)(H₂O)₄]Cl·2·H₂O complex (**6**)

Pale green solid. Yield: 71%. IR (KBr, ν/cm^{-1}): $\nu(\text{OH, NH and H}_2\text{O})$ 3432br&s, $\nu(\text{C=O})$ 1639s, $\nu(\text{C=N})$ 1607s, $\nu(\text{C=C})$ 1535 m, $\nu(\text{C-O})$ 1261 m, FT-IR(KBr, ν/cm^{-1}): $\nu(\text{Cu-O})$ 490 m, $\nu(\text{Cu-N})$ 385 m, $\nu(\text{Cu-Cl})$ 327 m. Molar conductance $\Delta\text{m}(\Omega^{-1}\text{cm}^2\text{mol}^{-1}) = 75$. TG: showed weight loss of 5.87% in temperature range 25–100 °C, calc. for 2(H₂O), 5.92% corresponding to dehydration process [Cu(HL¹)(H₂O)₄]Cl₂·H₂O → [Cu(HL¹)(H₂O)₄]Cl. Also, TG: found weight loss of 11.54% in temperature range 100.5–204 °C, calcd. for 4(H₂O), 11.84% corresponding to dehydration process of coordinated water [Cu(HL¹)(H₂O)₄]Cl → [Cu(HL¹)]Cl. Anal. Calcd for C₂₂H₂₈ClCuN₃O₁₁: C, 43.35; H, 4.63; Cl, 5.82; Cu, 10.43; N, 6.89. Found; C, 43.47; H, 4.86; N, 6.75.

4.1.8. (2-(1H-benzofurimidazol-2-yl)-4-(6-hydroxy-4,7-dimethoxybenzofuran-5-carbonyl)-1H-pyrrol-1-yl)iron(III) chloride tetrahydrate; [Fe(HL¹)Cl₂(H₂O)₂]·2·H₂O complex (**7**)

Dark brown solid. Yield: 78%. IR (KBr, ν/cm^{-1}): $\nu(\text{OH, NH and H}_2\text{O})$ 3571–3159s., $\nu(\text{C=O})$ 1642s, $\nu(\text{C=N})$ 1581s, $\nu(\text{C-O})$ 1266s, $\nu(\text{Fe-O})$ 670 m, $\nu(\text{Fe-Cl})$ 590 m. Molar conductance $\Delta\text{m}(\Omega^{-1}\text{cm}^2\text{mol}^{-1}) = 23$. TG: found weight loss of 5.81% in temperature range 25–100 °C, calc. for 2(H₂O), 6.0% corresponding to dehydration process [Fe(HL¹)Cl₂(H₂O)₂]·2H₂O → [Fe(HL¹)Cl₂(H₂O)₂]. Also, TG: showed weight loss of 6.21% in temperature range 100.5–204 °C, calcd. for 2(H₂O), 6.0% corresponding process to dehydration of coordinated water [Fe(HL¹)Cl₂(H₂O)₂] → [Fe(HL¹)Cl₂]. Anal. Calcd for C₂₂H₂₄Cl₂FeN₃O₉: C, 43.95; H, 4.02; Cl, 11.79; Fe, 9.29; N, 6.99. Found: C, 43.81; H, 4.23; Cl, 11.99; Fe, 9.03; N, 6.74.

4.1.9. (2-(1H-benzofurimidazol-2-yl)-4-(6-hydroxy-4,7-dimethoxybenzofuran-5-carbonyl)-1H-pyrrol-1-yl)zinc(II) chloride hydrate; [Zn(HL¹)Cl(H₂O)] complex (**8**)

Greenish yellow solid. Yield: 76%. ¹H-NMR (500 MHz, DMSO- *d*₆): 3.89(s, 3H, CH₃), 3.97(s, 3H, CH₃), 7.17(m, 4H, H3 benzofuran, H5' and H6' benzimidazole, H4'' pyrrol), 7.20(m, 1H, H7 benzimidazole), 7.44(m, 1H, H4' benzimidazole), 7.91 (d, 1H, *J* = 1.5 Hz, H2 benzofuran), 8.17(s, 1H, H2'' pyrrol), 12.59(br, NH benzimidazole D₂O exchangeable), 12.69(s, 1H, OH, D₂O exchangeable). ¹³C-NMR (500 MHz, DMSO-*d*₆): 61.1 (OCH₃), 61.45 (OCH₃), 106.12, 112.28, 114.15, 115.81, 118.03, 118.24, 125.79, 129.14, 129.45, 131.01, 132.43, 142.01, 144.35, 144.89, 145.37(Ar-C), 155.76(C=N), 188.37(C=O). IR (KBr, ν/cm^{-1}): $\nu(\text{OH, NH and H}_2\text{O})$ 3201br $\nu(\text{CH, aromatic})$ 3128 m, $\nu(\text{CH, aliphatic})$ 2978 m, $\nu(\text{C=O})$ 1641 s, $\nu(\text{C=N})$ 1615s, $\nu(\text{C=C})$ 1529 m, $\nu(\text{C-O})$ 1265s. FT-IR (KBr, ν/cm^{-1}): $\nu(\text{Zn-N})$ 465 m, $\nu(\text{Zn-Cl})$ 390 m. Molar conductance $\Delta\text{m}(\Omega^{-1}\text{cm}^2\text{mol}^{-1}) = 16$. TG: showed no weight loss in temperature range 25–100 °C, whereas, TG: found weight loss of 3.69% weight in temperature range 100.5–204 °C calcd. for (H₂O), 3.46% corresponding to dehydration process [Zn(HL¹)Cl(H₂O)] → [Zn(HL¹)Cl]. Anal. Calcd for C₂₂H₁₈ClN₃O₆Zn: C, 50.69; H, 3.48; Cl, 6.80; N, 8.06; Zn, 12.55. Found: C, 50.42; H, 3.51; Cl, 6.69; N, 8.35; Zn, 12.32.

4.1.10. Bis(2-(1H-benzofurimidazol-2-yl)-4-(6-hydroxy-4,7-dimethoxybenzofuran-5-carbonyl)-1H-pyrrol-1-yl)lanthanum(III) chloride pentahydrate [La(HL¹)₂(H₂O)₂]Cl₃·H₂O complex (**9**)

Pale green solid. Yield: 71%. ¹H-NMR (500 MHz, DMSO- *d*₆): 3.90 (s, 3H, CH₃), 3.95(s, 3H, CH₃), 7.17(m, 4H, H3 benzofuran, H5' and H6' benzimidazole, H4'' pyrrol), 7.22(m, 1H, H7 benzimidazole), 7.39(m, 1H, H4 benzimidazole), 7.91 (d, 1H, *J* = 1.5 Hz, H2 benzofuran), 8.15(s, 1H, H2'' pyrrol), 11.90(br, NH benzimidazole D₂O exchangeable), 13.07(s, 1H, OH, D₂O exchangeable). ¹³C-NMR (200 MHz, DMSO-*d*₆): 61.1 (OCH₃), 61.47 (OCH₃), 106.5, 112.21,

114.13, 115.91, 118.03, 118.31, 126.12, 128.87, 129.20, 131.31, 132.21, 143.11, 144.44, 145.02, 145.48, 152.81(C=N), 188.41(C=O). IR (KBr, ν/cm^{-1}): $\nu(\text{OH}, \text{NH}$ and $\text{H}_2\text{O})$ 3503–3165s, $\nu(\text{C}=\text{O})$ 1641s, $\nu(\text{C}=\text{N})$ 1579s, $\nu(\text{C}-\text{O})$ 1261s, FT-IR (KBr, ν/cm^{-1}): $\nu(\text{La}-\text{N})$ 470 m, $\nu(\text{La}-\text{Cl})$ 390 m. Molar conductance Δm ($\Omega^{-1}\text{cm}^2\text{mol}^{-1}$) = 68. TG: found weight loss of 5.23% in temperature range 25–100 °C, calcd. for 3 (H_2O), 5.05% corresponding to dehydration process $[\text{La}(\text{HL}^1)_2(\text{H}_2\text{O})_2]\text{Cl}\cdot 3\text{H}_2\text{O} \rightarrow [\text{La}(\text{HL}^1)_2(\text{H}_2\text{O})_2]\text{Cl}$. Also, TG: exhibited weight loss of 3.57% in temperature range 100.5–204 °C, calcd. for 2 (H_2O), 3.37% corresponding to dehydration of coordinated water process $[\text{La}(\text{HL}^1)_2(\text{H}_2\text{O})_2]\text{Cl} \rightarrow [\text{La}(\text{HL}^1)_2]\text{Cl}$. Anal. Calcd. for $\text{C}_{44}\text{H}_{42}\text{ClLaN}_6\text{O}_{15}$: C, 49.43; H, 3.96; Cl, 3.32; La, 12.99; N, 7.86;. Found: C, 49.71; H, 3.81; Cl, 3.22; La, 12.78; N, 7.98.

4.1.11. (3-(6-hydroxy-4,7-dimethoxybenzofuran-5-carbonyl)-8-oxo-8H-pyrimido[1,6-a]pyrimidin-6-yloxy)copper(II) chloride trihydrate [Cu(HL²)Cl(H₂O)₂] \cdot H₂O complex (10)

Yield: 75%. IR (KBr, ν/cm^{-1}): $\nu(\text{OH}, \text{H}_2\text{O})$ 3396br&s, $\nu(\text{C}=\text{O})$ 1691vs, $\nu(\text{C}=\text{O})$ 1641s, $\nu(\text{C}=\text{N})$ 1609 m, $\nu(\text{C}-\text{O})$ 1274 m, $\nu(\text{C}-\text{O})$ 1214s. FT-IR(KBr, ν/cm^{-1}): $\nu(\text{Cu}-\text{O})$ 485 m, $\nu(\text{Cu}-\text{N})$ 395 m, $\nu(\text{Cu}-\text{Cl})$ 325 m. Molar conductance Δm ($\Omega^{-1}\text{cm}^2\text{mol}^{-1}$) = 28. TG: found weight loss of 3.43% in temperature range 25–100 °C, calcd. for 1(H_2O), 3.37% corresponding to dehydration process $[\text{Cu}(\text{HL}^2)\text{Cl}(\text{H}_2\text{O})_2]\cdot\text{H}_2\text{O} \rightarrow [\text{Cu}(\text{HL}^2)\text{Cl}(\text{H}_2\text{O})_2]$. Also, TG: found weight loss of 6.77% in temperature range 100.5–204 °C, calcd. for 2(H_2O), 6.74% corresponding to dehydration of coordinated water process $[\text{Cu}(\text{HL}^2)\text{Cl}(\text{H}_2\text{O})_2] \rightarrow [\text{Cu}(\text{HL}^2)\text{Cl}]$. Anal. Calc. for $\text{C}_{18}\text{H}_{18}\text{ClCuN}_3\text{O}_{10}$: C, 40.38; H, 3.39; Cl, 6.62; Cu, 11.87; N, 7.85. Found: C, 40.03; H, 3.28; Cl, 6.52; Cu, 11.69; N, 7.51.

4.1.12. (3-(6-hydroxy-4,7-dimethoxybenzofuran-5-carbonyl)-8-oxo-8H-pyrimido[1,6-a]pyrimidin-6-yloxy)iron(III) chloride pentahydrate; [Fe(H₂L²)Cl \cdot (H₂O)₂] \cdot 2Cl \cdot 3H₂O (11)

Yield: 76%. IR (KBr, ν/cm^{-1}): $\nu(\text{OH})$ 3509br, $\nu(\text{NH}, \text{H}_2\text{O})$ 3409–3208br, $\nu(\text{C}=\text{O})$ 1709s, $\nu(\text{C}=\text{O})$ 1655s, $\nu(\text{C}=\text{O})$ 1641s, $\nu(\text{C}=\text{N})$ 1606s, $\nu(\text{C}-\text{O})$ 1213s. FT-IR(KBr, ν/cm^{-1}): $\nu(\text{Fe}-\text{O})$ 660, $\nu(\text{Fe}-\text{N})$ 480, $\nu(\text{Fe}-\text{Cl})$ 397. Molar conductance Δm ($\Omega^{-1}\text{cm}^2\text{mol}^{-1}$) = 67. TG: found weight loss of 8.21% in temperature range 25–100 °C, calcd. for 3(H_2O), 8.52% corresponding to dehydration process $[\text{Fe}(\text{H}_2\text{L}^2)\text{Cl}\cdot(\text{H}_2\text{O})_2]\cdot 2\text{Cl}\cdot 3\text{H}_2\text{O} \rightarrow [\text{Fe}(\text{H}_2\text{L}^2)\text{Cl}\cdot(\text{H}_2\text{O})_2]\cdot 2\text{Cl}$. Also, TG: found weight loss of 5.41% in temperature range 100.5–204 °C, calcd. for 2 (H_2O), 5.68% corresponding to dehydration process of coordinated water $[\text{Fe}(\text{H}_2\text{L}^2)\text{Cl}\cdot(\text{H}_2\text{O})_2]\cdot 2\text{Cl} \rightarrow [\text{Fe}(\text{H}_2\text{L}^2)\text{Cl}]\cdot 2\text{Cl}$. Anal. Calcd. for $\text{C}_{18}\text{H}_{23}\text{Cl}_3\text{FeN}_3\text{O}_{12}$: C, 34.01; H, 3.65; Cl, 16.73; Fe, 8.79; N, 6.61. Found: C, 33.93; H, 3.33; Cl, 16.65; Fe, 8.91; N, 6.36.

4.1.13. Bis-(6-hydroxy-4,7-dimethoxybenzofuran-5-carbonyl)-8-oxo-8H-pyrimido[1,6-a]pyrimidin-6-yloxy)cobalt(III) chloride dihydrate [Co(H₂L²)₂] \cdot 3Cl \cdot 2 \cdot H₂O (12)

Yield: 85%. ¹H-NMR (270 MHz, DMSO-*d*₆): 3.85(s, 3H, OCH₃), 3.93(s, 3H, OCH₃), 7.18(d, 1H, *J* = 2 Hz, H3 benzofuran), 7.96(d, 1H, *J* = 2 Hz, H2 benzofuran), 8.30(s, 1H, H4' pyrimidopyrimidinone), 8.93(s, 1H, H9' pyrimidopyrimidinone), 9.56(s, 1H, H2 pyrimidopyrimidinone), 11.67 (s, 1H, NH, D₂O exchangeable), 12.16(s, 1H, OH, D₂O exchangeable). ¹³C-NMR(270 MHz, DMSO-*d*₆): 61.24 (OCH₃), 60.83(OCH₃), 105.53, 108.11, 109.65, 110.78, 111.38, 112.12, 114.34, 127.17, 128.27, 135.92, 136.69, 143.15, 143.82, 144.31, 144.53, 145.08, 144.96 (C=O), 153.56, 157.15, 158.23(C=N), 161.26 (C=O), 191.37(C=O). IR (KBr, ν/cm^{-1}): $\nu(\text{OH}, \text{and } \text{H}_2\text{O})$ 3397br&s, $\nu(\text{NH})$ 3164br&s, $\nu(\text{CH}, \text{aromatic})$ 3061 m, 2931.36 (CH, aliphatic), $\nu(\text{C}=\text{O}, \text{amide})$ 1734s, $\nu(\text{C}=\text{O}, \text{amide})$ 1682s, $\nu(\text{C}=\text{O})$ 1641s, 1610 $\nu(\text{C}=\text{N})$ s, $\nu(\text{C}-\text{O})$ 1210s. FT-IR(KBr, ν/cm^{-1}): $\nu(\text{Co}-\text{O})$ 475, $\nu(\text{Co}-\text{N})$ 370. Molar conductance Δm ($\Omega^{-1}\text{cm}^2\text{mol}^{-1}$) = 79. TG: found weight loss of 3.58% in temperature range 25–100 °C, calcd. for 2(H_2O), 3.73% corresponding to dehydration process $[\text{Co}(\text{H}_2\text{L}^2)_2]\cdot 3\text{Cl}\cdot 2\cdot\text{H}_2\text{O} \rightarrow [\text{Co}(\text{H}_2\text{L}^2)_2]\cdot 3\text{Cl}$. Also, TG:

found no weight loss of coordinated water in temperature range 100.5–204 °C. Anal. Calcd. for $\text{C}_{36}\text{H}_{30}\text{Cl}_3\text{CoN}_6\text{O}_{16}$: C, 44.67; H, 3.12; Cl, 10.99; Co, 6.09; N, 8.68. Found: C, 44.32; H, 3.08; Cl, 10.71; Co, 6.32; N, 8.39.

4.1.14. (3-(6-hydroxy-4,7-dimethoxybenzofuran-5-carbonyl)-8-oxo-8H-pyrimido[1,6-a]pyrimidin-6-yloxy)lanthanum(III) chloride hydrate; [La(H₂L²)₂] \cdot 3Cl \cdot H₂O complex (13)

Yield: 66%. ¹H-NMR (270 MHz, DMSO-*d*₆): 3.85(s, 3H, OCH₃), 3.96(s, 3H, OCH₃), 7.17(d, 1H, *J* = 2 Hz, H3 benzofuran), 7.95(m, 3H, H2 benzofuran, H4' pyrimidopyrimidinone, H9' pyrimidopyrimidinone), 8.42(s, 1H, H2' pyrimidopyrimidinone), 10.35 (s, 1H, NH, D₂O exchangeable), 12.16(s, 1H, OH, D₂O exchangeable). ¹³C-NMR(270 MHz, DMSO-*d*₆): 61.26, 60.83, 105.55, 108.11, 109.70, 110.98, 111.41, 112.09, 114.42, 127.08, 128.41, 136.52, 137.79, 143.21, 143.98, 144.65, 144.99, 145.63, 146.46(C=O), 153.44, 157.29, 158.57 (C=N), 161.98(C=O), 191.37(C=O). IR (KBr, ν/cm^{-1}): $\nu(\text{OH}, \text{NH}$ and $\text{H}_2\text{O})$ 3362br., $\nu(\text{NH})$ 3160b, $\nu(\text{CH}, \text{aromatic})$ 3026 m, 2936 (CH, aliphatic), $\nu(\text{C}=\text{O}, \text{amide})$ 1738s, $\nu(\text{C}=\text{O}, \text{amide})$ 1672s, $\nu(\text{C}=\text{O})$ 1639s, $\nu(\text{C}=\text{N})$ 1607s, $\nu(\text{C}-\text{O})$ 1213s, $\nu(\text{La}-\text{O})$ 650 m, $\nu(\text{La}-\text{N})$ 475 m. Molar conductance Δm ($\Omega^{-1}\text{cm}^2\text{mol}^{-1}$) = 85. TG: found weight loss of 1.91% in temperature range 25–100 °C, calcd. for 2(H_2O), 1.75% corresponding to dehydration process $[\text{La}(\text{H}_2\text{L}^2)_2]\cdot 3\text{Cl}\cdot\text{H}_2\text{O} \rightarrow [\text{La}(\text{H}_2\text{L}^2)_2]\cdot 3\text{Cl}$. Also, TG: found no loss of coordinated water in temperature range 100.5–204 °C. Anal. Calc. for $\text{C}_{36}\text{H}_{28}\text{Cl}_3\text{LaN}_6\text{O}_{15}$: C, 41.98; H, 2.74; Cl, 10.33; La, 13.49; N, 8.16. Found: C, 42.08; H, 2.67; Cl, 10.64; La, 13.56; N, 8.25.

4.2. Biological assays

4.2.1. HIV inhibitory activity and reverse transcriptase inhibition with therapeutic windows

4.2.1.1. Materials and methods

4.2.1.1.1. Cells and viruses. CEM-SS cells, laboratory-derived virus isolates (including drug-resistant virus isolates), and low-passage clinical virus isolates used in these evaluations were previously described in detail [25]. These cells were maintained in RPMI 1640 medium supplemented with 10% fetal bovine serum, 2 μM glutamine, penicillin (100 U/mL), and streptomycin (100 $\mu\text{g}/\text{mL}$). Fresh human cells were obtained from the American Red Cross (Baltimore, Md.).

4.2.1.1.2. Antiviral and cross-resistance assays. The inhibitory activities of the tested compounds against HIV were evaluated by microtiter anti-HIV assays with CEM-SS cells or fresh human peripheral blood mononuclear cells (PBMCs); these assays quantify the ability of a compound to inhibit HIV-induced cell killing or HIV replication. Quantification was performed by the tetrazolium dye XTT assay, which is metabolized to a colored formazan product by viable cells. Antiviral and toxicity data were reported as the quantity of drug required to inhibit virus-induced cell killing or virus production by 50% (EC₅₀).

4.2.1.1.3. Reverse transcriptase (RT) enzyme inhibition assays. Each of the newly synthesized compounds was tested for RT inhibitory activity against purified recombinant HIV-1 RT using the cell-free Quan-T-RT assay system (Amersham Corp., Arlington Heights, IL), which utilizes the scintillation proximity assay (SPA) principle [26,27]. In the assay, a DNA/RNA template is bound to SPA beads via a biotin/streptavidin linkage. The primer DNA is a 16-meroligo (T), which has been annealed to a poly(rA) template. The primer-template is bound to a streptavidin-coated SPA bead. [³H] TTP (thymidine 5' triphosphate) is incorporated into the primer by reverse transcription. In brief, [³H]TTP, at a final concentration of 0.5 $\mu\text{Ci}/\text{sample}$, was diluted in RT assay buffer (49.5 μM Tris-HCl, pH 8.0, 80 μM KCl, 10 μM MgCl₂, 10 μM dithiothreitol, 2.5 μM EGTA, 0.05% Nonidet P-40) and added to annealed DNA/RNA bound to SPA

beads. The compound being tested was added to the reaction mixture at 0.001–100 μM concentrations. Addition of 10 μU of recombinant HIV RT and incubation at 37 °C for 1 h resulted in the extension of the primer by incorporation of [^3H]TTP. The reaction was stopped by addition of 0.2 mL of 120 μM EDTA. The samples were counted in an open window using a Beckman LS 7600 instrument and $\text{IC}_{50[\text{RT}]}$ values (concentration at which the compound inhibits recombinant RT by 50%) were calculated by comparing the measurements to untreated sample.

4.3. Hepatitis C virus (HCV) NS3-4A protease inhibitory activity

4.3.1. Materials and methods

4.3.1.1. Cells. Parental Huh-7 and HepG2 cells were cultured in Dulbecco's modified Eagle's medium (DMEM) containing 10% heat-inactivated fetal bovine serum (FBS), 2 μM L-glutamine, and nonessential amino acids. Stable Huh-7 cells containing the self-replicating, subgenomic HCV replicon, which was identical in sequence to the I₃₇₇neo/NS3-3'/wt replicon described by Lohmann et al. [28], were selected and maintained in the presence of 0.25 mg/mL G418 (Invitrogen, Carlsbad, CA) and were used for anti-HCV assays. Peripheral blood mononuclear cells (PBMC) were isolated from fresh donor blood and cultured in RPMI-1640 medium (JRH Biosciences).

4.3.1.2. Determination of anti-HCV activity and cytotoxicity. Determination of 50% inhibitory concentration (IC_{50}), 90% inhibitory concentration (IC_{90}), and 50% cytotoxic concentration (CC_{50}) of all the tested compounds in HCV replicon cells was performed [29,30]. Briefly, 1×10^4 replicon cells per well were plated in 96-well plates. On the following day, replicon cells was incubated at 37 °C for the indicated period of time with antiviral agents serially diluted in DMEM plus 2% FBS and 0.5% dimethyl sulfoxide (DMSO). Total cellular RNA was extracted using an RNeasy-96 kit (QIAGEN, Valencia, CA), and the copy number of HCV RNA was determined using a quantitative RT-PCR (QRT-PCR) assay [30]. Each datum point represents the average of five replicates in cell culture.

The cytotoxicity of the tested compounds was measured under the same experimental settings using a tetrazolium (MTS)-based cell viability assay (Promega, Madison, WI). For the cytotoxicity assay with human hepatocyte cell lines, 1×10^4 parental Huh-7 cells per well or 4×10^4 HepG2 cells per well were used. To determine cytotoxicity of the tested compound against resting PBMC, 1×10^5 cells per well were incubated with the tested compound in RPMI-1640 medium (no serum) for 48 h, and the cell viability was determined by the MTS-based assay. To determine cytotoxicity of the tested compound against proliferating PBMC, 1×10^5 cells per well in RPMI-1640 medium were added to a 96-well plate, which was pre-coated with anti-human CD3 antibody (Accurate Chemical & Scientific Corporation, Westbury, NY). The cells were incubated with the tested compound and anti-human CD28 antibody (PharMingen/BD Biosciences, San Jose, CA) for 72 h at 37 °C, and the cell growth was determined by [^3H] thymidine uptake between the 48th and 72nd h.

4.4. Determination of the median lethal dose LD_{50}

The median lethal dose of the tested compounds was determined according to the procedure described by Lorke [31–33]. The experiment was carried out on two phases; the first phase involved three groups of three animals per each group. One dose was given to each group intraperitoneally and the treated mice were monitored for 24 h for mortality and general behaviors. The second phase comprises 3–4 groups of one mouse per group were given

doses, based on the findings of phase 1, the mice were again monitored for 24 h. The geographic mean of the least dose that killed mice and the highest dose that did not kill mice was taken as the median lethal dose.

Acknowledgements

The authors express their deep thanks to “**Sanofi-Aventis (Paris, FR)**” for the evaluation of: the HIV & HIV RT inhibitory activity, the HCV NS3-4A protease inhibitor activity and the median lethal dose of the synthesized compounds and we also thank Dr. Mohamed M. Abdalal.

References

- [1] X.L. Hou, Z. Yang, H.N.C. Wong, Furans and Benzofurans. in: G.W. Gribble, T. L. Gilchrist (Eds.), Progress in Heterocyclic Chemistry, vol. 14. Pergamon, Oxford, 2002, pp. 139–179.
- [2] A. Mustafa, Furoprans and Furoprones. John Wiley and Sons, Inc., NY, 1967, 102–159.
- [3] R.B. Gammill, B.R. Hyde, J. Org. Chem. 48 (1983) 3863–3865.
- [4] S. Kim, A.A. Salim, S.M. Swanson, A.D. Kinghorn, Anticancer Agents Med. Chem. 6 (2006) 319–345 [My paper].
- [5] R. Whomsley, E. Fernandez, P.J. Nicholls, H.J. Smith, P. Lombardi, V. Pestellini, J. Steroid Biochem. Mole. Biol. 44 (1993) 675–676.
- [6] S.M. Rida, S.A.M. El-Hawash, H.T.Y. Fahmy, A.A. Hazza, M.M.M. El-Meligy, Arch. Pharm. Res. 29 (2006) 16–25.
- [7] I. Hayakawa, R. Shioya, T. Agatsuma, Y. Sugano, Chem. Pharm. Bull. 53 (2005) 638–640.
- [8] S.A. Galal, A.S. Abd El-Ali, M.M. Abdallah, H.I. El-Diwani, Bioorg. Med. Chem. Lett. 19 (2009) 2420–2428.
- [9] J. Kona, W.M.F. Fabian, P. Zahrndnik, J. Chem. Soc., Perkin. Trans. 2 (2001) 422–426.
- [10] F. Ati, S. El-Aoufi, A. Chergui, H.Y. Aboul-Enein, B. Maouche, J. Iran. Chem. Soc. 5 (3) (2008) 506–513.
- [11] D.W. Rodgers, S.J. Gamblin, B.A. Harris, S. Ray, J.S. Culp, B. Hellmig, D.J. Woolf, C. Debouck, S.C. Harrison, Proc. Natl. Acad. Sci. U.S.A. 92 (1995) 1222–1226.
- [12] R. De Francesco, L. Tomei, S. Altamura, V. Summa, G. Migliaccio, Antiviral Res. 58 (2003) 1–16.
- [13] R. De Francesco, A. Pessi, C. Steinkuhler, J. Viral Hepat. 6 (1999) 23–30.
- [14] S.A. Galal, K.H. Hegab, A.S. Kassab, M.L. Rodriguez, S.M. Kerwin, A.A. El-Khamry, H.I. El Diwani, Eur. J. Med. Chem. 44 (2009) 1500–1508.
- [15] H. Hagen, G. Nilz, H. Walter, A. Landes, F. Wolfgang, Patent US 542, 0307 (1995).
- [16] F. Eiden, G. Radenmacher, J. Schuenemann Archiv der Pharmazie 316 (1983) 34–42.
- [17] L.A. Cescon, A.R. Day, J. Org. Chem. 27 (1962) 581–586.
- [18] J. Garin, E. Meléndez, F.L. Merchán, D. Ortiz, T. Tejero, Synthesis (1987) 368–370.
- [19] J.R. Ferraro, Low-frequency Vibrations of Inorganic and Coordination Compounds. Plenum Press, New York, 1971, pp. 194–197.
- [20] K. Husain, M. Abid, A. Azam, Eur. J. Med. Chem. 42 (2007) 1300–1308.
- [21] S.S. Kandil, G.Y. Ali, A. El-Dissouky, Transition Met. Chem. 27 (2002) 398–406.
- [22] D. Kovala-Demertzi, A. Boccarelli, M.A. Demertzi, M. Coluccia, Chemotherapy 53 (2007) 148–152.
- [23] E. Ispir, M. Kurtoglu, F. Purtaş, S. Serin, Transition Met. Chem. 30 (2005) 1042–1047.
- [24] D.X. West, C.S. Carlson, A.E. Liberta, Transition Met. Chem. 16 (1991) 53–56.
- [25] R.W. Buckheit, T.L. Kinjerski, V. Fliakas-Boltz, J.D. Russell, T.L. Stup, L. A. Pallansch, W.G. Brouwer, D.C. Dao, W.A. Harrison, R.J. Schultz, J.P. Bader, S. S. Yang, Antimicrob. Agents Chemother. 39 (1995) 2718–2727.
- [26] J.M. Zarling, P.A. Moran, O. Haffar, M. Diegel, D.E. Myers, V. Kuelbeck, J. A. Ledbetter, F.M. Uckun, Int. J. Immunopharmacol. 13 (1991) 63–68.
- [27] N. Bosworth, P. Towers, Nature 341 (1989) 167–168.
- [28] V. Lohmann, F. Körner, J.O. Koch, U. Herian, L. Theilmann, R. Bartschlagler, Science 285 (1999) 110–113.
- [29] K. Lin, A.D. Kwong, C. Lin, Antimicrob. Agents Chemother. 48 (2004) 4784–4792.
- [30] R.B. Perni, S.J. Almquist, R.A. Byrn, G. Chandorkar, P.R. Chaturvedi, L. F. Courtney, C.J. Decker, K. Dinehart, C.A. Gates, S.L. Harbeson, A. Heiser, G. Kalkeri, E. Kolaczowski, K. Luong, Y.P. Rao, B.G. Taylor, W.P. Thomson, J. A. Tung, R.D. Wei, Y. Kwong, A.D. Lin, C. Lin, Antimicrob. Agents Chemother. 50 (2006) 899–909.
- [31] D. Lorke, Arch. Toxicol. 54 (1983) 275–287.
- [32] P.A. Akah, A.C. Ezike, S.V. Nwafor, C.O. Okoli, N.M. Enwerem, J. Ethnopharmacol. 89 (2003) 25–36.
- [33] P.O. Osadebe, F.B.C. Okoye, J. Ethnopharmacol. 89 (2003) 19–24.